SCIENCE CHINA
Mathematics

• ARTICLES •

June 2013 Vol. 56 No. 6: 1287–1300
doi: 10.1007/s11425-013-4584-2

Moving finite element methods for time fractional partial differential equations

JIANG YingJun[1,*] & MA JingTang[2]

[1]*Department of Mathematics and Scientific Computing, Changsha University of Science and Technology, Changsha 410076, China;*
[2]*School of Economic Mathematics, Southwestern University of Finance and Economics, Chengdu 611130, China*
Email: jiangyingjun@csust.edu.cn, mjt@swufe.edu.cn

Received July 7, 2012; accepted December 17, 2012; published online February 5, 2013

Abstract With the aim of simulating the blow-up solutions, a moving finite element method, based on nonuniform meshes both in time and in space, is proposed in this paper to solve time fractional partial differential equations (FPDEs). The unconditional stability and convergence rates of $2-\alpha$ for time and r for space are proved when the method is used for the linear time FPDEs with α-th order time derivatives. Numerical examples are provided to support the theoretical findings, and the blow-up solutions for the nonlinear FPDEs are simulated by the method.

Keywords fractional partial differential equations, moving finite element methods, blow-up solutions

MSC(2010) 65M60, 65M12, 65M06, 35S10, 65R20

Citation: Jiang Y J, Ma J T. Moving finite element methods for time fractional partial differential equations. Sci China Math, 2013, 56: 1287–1300, doi: 10.1007/s11425-013-4584-2

1 Introduction

Showing a lot of advantages in modeling anomalous diffusion processes found ubiquitously in the natural world, fractional partial differential equations (FPDEs) attract much attention from a variety of fields (see e.g., [5,18]). Generally, FPDEs can be divided into three types: time fractional partial differential equations, space fractional partial differential equations and space-time fractional partial differential equations. This paper, based on nonuniform meshes, numerically solves the following linear time fractional partial differential equation,

$$\frac{\partial^\alpha u(x,t)}{\partial t^\alpha}-\frac{\partial^2 u(x,t)}{\partial x^2}=f(x,t),\quad x\in I:=(0,1),\quad t\in J:=(0,T), \tag{1.1}$$

subject to the initial and boundary conditions:

$$u(x,0)=u_0(x),\quad x\in I, \tag{1.2}$$

$$u(0,t)=u(1,t)=0,\quad t\in J, \tag{1.3}$$

where $0<\alpha<1$, f and u_0 are given smooth functions, $\frac{\partial^\alpha u(x,t)}{\partial t^\alpha}$ is the Caputo fractional derivative defined by

$$\frac{\partial^\alpha u(x,t)}{\partial t^\alpha}=\frac{1}{\Gamma(1-\alpha)}\int_0^t\frac{\partial u(x,s)}{\partial s}\frac{ds}{(t-s)^\alpha}, \tag{1.4}$$

*Corresponding author

and $\Gamma(z) = \int_0^\infty \mathrm{e}^{-t} t^{z-1} dt$ is the gamma function. The problem has been used to model the sub-diffusion processes with the asymptotic behavior of their mean square displacement as a function of time

$$\langle x^2(t) \rangle \sim t^\alpha \tag{1.5}$$

(see [18]).

Many scholars have been making efforts on numerical solutions to problem (1.1)–(1.3) (see [9, 12, 13, 17, 19]). Among them, Lin and Xu [13] studied finite difference methods for time and spectral methods for space. In their work, the first-order derivative in the integrand of Caputo definition is discretised by a finite difference quotient, and the following form for approximation of the time fractional derivative operator, after calculating the coefficients and re-arranging the indices, is derived:

$$\frac{\partial^\alpha u(x,t)}{\partial t^\alpha} \approx \frac{1}{\Gamma(2-\alpha)} \sum_{j=0}^{k} b_j \frac{u(x, t_{k+1-j}) - u(x, t_{k-1})}{(\Delta t)^\alpha}.$$

Li and Xu [12] studied Galerkin spectral methods where Riemann-Liouville definition is used to define the time fractional derivatives. McLean and Mustapha [17], Mustapha and McLean [19] developed discontinuous Galerkin time-stepping methods for time FPDEs.

Another type of time FPDEs that should be mentioned here is

$$u_t = \frac{\partial^\alpha u_{xx}}{\partial t^\alpha} + f(x,t),$$

which is a simple form of Fokker-Planck equation and can be converted into (1.1) under certain conditions (see [12]). This equation is widely studied by scholars as well. Deng [11] used predictor-corrector approach originally developed for fractional ODEs (see e.g., [3, 4, 15]). The idea of his approach is that of transforming the equation into a Volterra integral equation with the use of Riemann-Liouville integrator and then discretizing the Volterra integral equation with finite difference methods. Chen et al. [2] designed an implicit finite difference scheme for time fractional derivatives and analyzed the stability and convergence using discrete Fourier methods, via the relationship between Grünwald-Letnikov and Riemann-Liouville fractional derivatives. Zhuang et al. [21] integrated the Fokker-Planck equation over temporal mesh and then used quadrature to calculate the integrals where finite difference methods are used to discretize the space. Zhuang et al. [22] studied a nonlinear Fokker-Planck equation, using a decoupling technique of decomposing the equation into a system of three equations and then extending the numerical schemes in [21] to the system.

The motivation of this paper is to simulate the blow-up solutions occurring in some nonlinear fractional partial differential equations (see [10]). Since the blowup solution $u(x,t)$ has sharp variations both in time and in space when t approaches to the blow-up time, we need to design stable and convergent numerical schemes based on nonuniform meshes in time and moving meshes in space. Yet moving mesh methods are mostly studied for integer-order partial differential equations and rarely for fractional partial differential equations (most references on convergence analysis and applications of moving mesh methods are included in the recent book by Huang and Russell [7]), and few literatures, to the best of our knowledge, concern the numerical solutions to time FPDEs based on nonuniform meshes, except for Ma and Jiang's work [16] in which they, with no analysis of the stability and convergence, developed moving collocation methods for simulating blow-up solutions to nonlinear time fractional partial differential equations. We design a moving finite element method for problem (1.1)–(1.3) based on nonuniform meshes in time and moving meshes in space in the present paper. In our method, the finite difference method is used to discretise the time derivatives, and we obtain the convergence of $O(\Delta t^{2-\alpha} + h^r)$ when the finite element space is the one consisting of the 3rd-order piecewise polynomials. The major contribution is as follows:

(1) Develop a technique, simple and applicable for the case with nonuniform time grids, to analyze the stability and convergence of the finite difference method used to discretize the time derivative in (1.1).

(2) Present a moving mesh method for the linear time FPDEs with theoretical analysis of its stability and convergence, and furthermore provide a way to simulate the blow-up solutions to the nonlinear time FPDEs with $f \equiv u^p,\ p > 1$.

In this paper, we assume the solution u is sufficiently smooth, and use the following norms: $\|v\| = \|v\|_{L^2(I)}$ and $\|v\|_r = \|v\|_{H^r(I)}$. C denotes a generic positive constant that does not depend on mesh but on T, α and the smoothness of u. The rest of this paper is organized as follows: in Section 2, the time derivative in (1.1) is estimated with the use of a finite difference method; in Section 3, a moving mesh finite method is presented and its stability and convergence are analyzed; in Section 4, numerical tests are carried out to support our theoretical findings, and the blow-up solutions for the nonlinear FPDEs are simulated by the method; in Section 5, conclusions are made.

2 Discretization of time fractional derivative operators

Define a time mesh

$$0 = t_0 < t_1 < \cdots < t_L = T,$$

and let

$$t_{n-1/2} = \frac{t_{n-1} + t_n}{2}, \quad \Delta t_n = t_n - t_{n-1}, \quad \Delta t = \max_{1 \leqslant n \leqslant L} \Delta t_n, \quad n = 0, 1, \ldots, L.$$

The time fractional derivative $\frac{\partial^\alpha u(x,t_n)}{\partial^\alpha t}$ can be formulated by

$$\begin{aligned} \frac{\partial^\alpha u(x,t_n)}{\partial t^\alpha} &= \frac{1}{\Gamma(1-\alpha)} \sum_{k=1}^{n} \int_{t_{k-1}}^{t_k} \frac{\partial u(x,s)}{\partial s} \frac{ds}{(t_n - s)^\alpha} \\ &= \frac{1}{\Gamma(1-\alpha)} \sum_{k=1}^{n} \frac{\partial}{\partial t} u(x, t_{k-1/2}) \int_{t_{k-1}}^{t_k} \frac{ds}{(t_n - s)^\alpha} + \gamma_1^{(n)}(x) \\ &= \frac{1}{\Gamma(1-\alpha)} \sum_{k=1}^{n} b_k^{(n)} \Delta u_k(x) + \gamma_1^{(n)}(x) + O(\Delta t^2), \end{aligned} \tag{2.1}$$

where

$$b_k^{(n)} = \frac{1}{\Delta t_k} \int_{t_{k-1}}^{t_k} \frac{ds}{(t_n - s)^\alpha}, \quad \Delta u_k(x) = u(x, t_k) - u(x, t_{k-1}), \quad 1 \leqslant k \leqslant n, \tag{2.2}$$

and

$$\gamma_1^{(n)}(x) = \frac{1}{\Gamma(1-\alpha)} \sum_{k=1}^{n} \int_{t_{k-1}}^{t_k} \left(\frac{\partial u(x,s)}{\partial s} - \frac{\partial}{\partial t} u(x, t_{k-1/2}) \right) \frac{ds}{(t_n - s)^\alpha}. \tag{2.3}$$

In the following we will estimate $b_k^{(n)}$ and $\gamma_1^{(n)}$.

Lemma 2.1. *We have the following estimations for* $b_k^{(n)}$,

$$b_{k-1}^{(n)} < b_k^{(n)}, \quad k = 2, \ldots, n, \quad n = 1, \ldots, L, \tag{2.4}$$

$$b_k^{(n)} < b_k^{(n-1)}, \quad k = 1, \ldots, n, \quad n = 2, \ldots, L, \tag{2.5}$$

$$b_1^{(n)} > t_n^{-\alpha}, \quad n = 1, \ldots, L. \tag{2.6}$$

Proof. The proof is straightforward by noting that $b_k^{(n)}$ is just the average of $(t_n - s)^{-\alpha}$ on $[t_{k-1}, t_k)$. □

To estimate $\gamma_1^{(n)}$, we need the following lemma.

Lemma 2.2. *There exists a positive* C *depending on* α *such that*

$$\left| \int_0^T s^{1-\alpha} ds - \sum_{k=1}^{L} \frac{\Delta t_k}{2} [t_{k-1}^{1-\alpha} + t_k^{1-\alpha}] \right| \leqslant C \Delta t^{2-\alpha}. \tag{2.7}$$

Proof. Since $\Delta t = \max_{1 \leqslant n \leqslant L} \Delta t_n$, there must be a mesh point t_i such that

$$2\Delta t \leqslant t_i < 3\Delta t. \tag{2.8}$$

Write

$$\int_0^T s^{1-\alpha}ds - \sum_{k=1}^{L}\frac{\Delta t_k}{2}[t_{k-1}^{1-\alpha}+t_k^{1-\alpha}] \equiv T_I + T_{II}$$

with

$$T_I := \int_0^{t_i} s^{1-\alpha}ds - \sum_{k=1}^{i}\frac{\Delta t_k}{2}[t_{k-1}^{1-\alpha}+t_k^{1-\alpha}]$$

and

$$T_{II} := \sum_{k=i+1}^{L}\bigg(\int_{t_{k-1}}^{t_k} s^{1-\alpha}ds - \frac{\Delta t_k}{2}[t_{k-1}^{1-\alpha}+t_k^{1-\alpha}]\bigg).$$

Using (2.8), we can derive

$$|T_I| \leqslant C\Delta t^{2-\alpha}. \tag{2.9}$$

Note that $\frac{\Delta t_k}{2}[t_{k-1}^{1-\alpha}+t_k^{1-\alpha}]$ is just the trapezoidal rule for the integral $\int_{t_{k-1}}^{t_k} s^{1-\alpha}ds$. Using

$$\frac{d^2}{ds^2}(s^{1-\alpha}) = -(1-\alpha)\alpha s^{-1-\alpha}$$

and the standard error estimation for trapezoidal rule, we have

$$\begin{aligned}|T_{II}| &\leqslant \sum_{k=i+1}^{L}\frac{\Delta t_k^3}{12}\max_{s\in[t_{k-1},t_k]}\bigg|\frac{d^2}{ds^2}(s^{1-\alpha})\bigg| \\ &\leqslant C\sum_{k=i+1}^{L}\frac{\Delta t_k^3}{t_{k-1}^{1+\alpha}} \leqslant C\Delta t^2\sum_{k=i+1}^{L}\frac{\Delta t_k}{t_{k-1}^{1+\alpha}}.\end{aligned} \tag{2.10}$$

For $s\in[t_{k-1},t_k]$, $k=i+1,\ldots,L$, we have

$$g(s) := \frac{1}{(s-\Delta t)^{1+\alpha}} \geqslant \frac{1}{(t_k-\Delta t)^{1+\alpha}} \geqslant \frac{1}{t_{k-1}^{1+\alpha}}. \tag{2.11}$$

Combining (2.11) with (2.10) gives

$$\begin{aligned}|T_{II}| &\leqslant C\Delta t^2\sum_{k=i+1}^{L}\int_{t_{k-1}}^{t_k} g(s)ds \leqslant C\Delta t^2\int_{2\Delta t}^{T} g(s)ds \\ &= \frac{C}{\alpha}\Delta t^2(\Delta t^{-\alpha}-(T-\Delta t)^{-\alpha}) \leqslant C\Delta t^{2-\alpha}.\end{aligned} \tag{2.12}$$

By (2.9) and (2.12), we obtain the estimation

$$\bigg|\int_0^T s^{1-\alpha}ds - \sum_{k=1}^{L}\frac{\Delta t_k}{2}[t_{k-1}^{1-\alpha}+t_k^{1-\alpha}]\bigg| \leqslant C\Delta t^{2-\alpha}.$$

Thus the proof of this lemma is complete. □

Lemma 2.3. *Let $\gamma_1^{(n)}(x)$ be given by* (2.3). *Then we have*

$$|\gamma_1^{(n)}(x)| \leqslant C\Delta t^{2-\alpha}. \tag{2.13}$$

Proof. Using Taylor's theorem, we can verify that

$$|\gamma_1^{(n)}(x)| \leqslant C\bigg|\sum_{k=1}^{n}\int_{t_{k-1}}^{t_k}\frac{t_{k-1/2}-s}{(t_n-s)^{\alpha}}ds\bigg| + O(\Delta t^2)$$

$$\leqslant C\left|\sum_{k=1}^{n}\int_{t_{k-1}}^{t_k}\frac{t_{k-1}+t_k-2s}{(t_n-s)^\alpha}ds\right|+O(\Delta t^2).$$

We estimate the first term on the right-hand side in the above equation as follows:

$$\begin{aligned}\sum_{k=1}^{n}\int_{t_{k-1}}^{t_k}\frac{t_{k-1}+t_k-2s}{(t_n-s)^\alpha}ds &= -\sum_{k=1}^{n}\frac{t_{k-1}+t_k}{1-\alpha}[(t_n-t_k)^{1-\alpha}-(t_n-t_{k-1})^{1-\alpha}]\\ &\quad+\sum_{k=1}^{n}\frac{2}{1-\alpha}[t_k(t_n-t_k)^{1-\alpha}-t_{k-1}(t_n-t_{k-1})^{1-\alpha}]\\ &\quad-\frac{2}{1-\alpha}\int_0^{t_n}(t_n-s)^{1-\alpha}ds\\ &=\frac{2}{1-\alpha}\sum_{k=1}^{n}\frac{\Delta t_k}{2}[(t_n-t_k)^{1-\alpha}+(t_n-t_{k-1})^{1-\alpha}]\\ &\quad-\frac{2}{1-\alpha}\int_0^{t_n}(t_n-s)^{1-\alpha}ds.\end{aligned}$$

Noting that

$$\sum_{k=1}^{n}\frac{\Delta t_k}{2}[(t_n-t_k)^{1-\alpha}+(t_n-t_{k-1})^{1-\alpha}]$$

is just the trapezoidal rule for

$$\int_0^{t_n}(t_n-s)^{1-\alpha}ds,$$

we have, by Lemma 2.2, that

$$\left|\sum_{k=1}^{n}\int_{t_{k-1}}^{t_k}\frac{t_{k-1}+t_k-2s}{(t_n-s)^\alpha}ds\right|\leqslant C\Delta t^{2-\alpha},$$

and thereby (2.13) is obtained. □

The following two lemmas are also crucial to the analysis of the stability and convergence of moving finite element methods.

Lemma 2.4. *Let M be an integer satisfying $1\leqslant M\leqslant L$, and μ be a positive number. If a series of positives ε_n, $n=0,1,\dots,M$, satisfy that*

$$b_n^{(n)}\varepsilon_n\leqslant\sum_{k=2}^{n}(b_k^{(n)}-b_{k-1}^{(n)})\varepsilon_{k-1}+b_1^{(n)}\mu,\quad n=1,\dots,M, \tag{2.14}$$

we have

$$\varepsilon_n\leqslant\mu,\quad n=1,\dots,M. \tag{2.15}$$

Proof. We prove the lemma by induction. It is direct to verify that $\varepsilon_1\leqslant\mu$. Suppose that (2.15) holds for $1\leqslant n\leqslant j-1$ with some $j\leqslant M$. By (2.14) we have

$$b_j^{(j)}\varepsilon_j=\sum_{k=2}^{j}(b_k^{(j)}-b_{k-1}^{(j)})\mu+b_1^{(j)}\mu\leqslant b_j^{(j)}\mu.$$

Therefore we obtain $\varepsilon_j\leqslant\mu$. □

Lemma 2.5. *Suppose that positives ε_n, $n=0,1,\dots,L$, satisfy*

$$b_n^{(n)}\varepsilon_n\leqslant\sum_{k=2}^{n}(b_k^{(n)}-b_{k-1}^{(n)})\varepsilon_{k-1}+b_1^{(n)}\mu+\kappa,\quad n=1,\dots,L, \tag{2.16}$$

where κ,μ are positives. Then we have

$$\varepsilon_M\leqslant\mu+\kappa/b_1^{(M)},\quad M=1,\dots,L. \tag{2.17}$$

Proof. For any integer M satisfying $1 \leqslant M \leqslant L$, by (2.5) and (2.16), we have

$$b_n^{(n)}\varepsilon_n \leqslant \sum_{k=2}^{n}(b_k^{(n)} - b_{k-1}^{(n)})\varepsilon_{k-1} + b_1^{(n)}(\mu + \kappa/b_1^{(M)}), \quad n = 1, \dots, M. \tag{2.18}$$

By Lemma 2.4, we obtain (2.17). □

3 Moving finite element methods

Let N be a positive integer, and define time-dependent spatial grids at time t_n $(n = 0, 1, \dots)$ by

$$0 = x_0^{(n)} < x_1^{(n)} < \cdots < x_N^{(n)} = 1.$$

Let

$$h^{(n)} := \max_{1 \leqslant k \leqslant N}(x_k^{(n)} - x_{k-1}^{(n)}), \quad h_n := \max_{0 \leqslant m \leqslant n} h^{(m)}.$$

Assume the mesh moving speed satisfies

$$|x_i^{(n)} - x_i^{(n-1)}| \leqslant C\Delta t_n, \quad i = 1, \dots, N-1, \quad n = 1, \dots, L. \tag{3.1}$$

Denote a piecewise polynomial space

$$V^{(n)} := \{v \in C(I):\ v|_{[x_k^{(n)}, x_{k+1}^{(n)}]} \in P_r,\ k = 0, 1, \dots, N-1\},$$

where P_r denotes the set of piecewise polynomials of degree not exceeding r. Insert in $[x_k^{(n)}, x_{k+1}^{(n)}]$ by $r-1$ points

$$x_{k+j/r}^{(n)} = x_k^{(n)} + \frac{j}{r}(x_{k+1}^{(n)} - x_k^{(n)}), \quad j = 1, \dots, r-1.$$

Define an interpolant operator

$$\Pi_r^{(n)}:\ C(I) \to V^{(n)},$$

with $\Pi_r^{(n)}|_{[x_k^{(n)}, x_{k+1}^{(n)}]}$ being an r-th order polynomial interpolant on

$$[x_k^{(n)}, x_{k+1}^{(n)}], \quad k = 0, 1, \dots, N-1,$$

associated with local grid points $x_{k+j/r}^{(n)}$, $j = 0, 1, \dots, r$.

The weak form of (1.1)–(1.3) is given by

$$\left(\frac{\partial^\alpha}{\partial t^\alpha}u, v\right) + a(u, v) = (f, v), \quad \forall\, v \in H_0^1(I), \tag{3.2}$$

where $(\cdot, \cdot)$ is the inner product in $L^2(I)$ and

$$a(u, v) = \int_I u_x v_x \, dx.$$

The moving finite element method is defined by: Find $U^{(n)}(x) \in V^{(n)}$, $n = 1, 2, \dots, L$, such that

$$b_n^{(n)}(U^{(n)}(x), v) + \Gamma(1-\alpha)a(U^{(n)}(x), v) = \sum_{k=2}^{n}(b_k^{(n)} - b_{k-1}^{(n)})(\widetilde{U}^{(k-1)}(x), v) + b_1^{(n)}(\widetilde{U}^{(0)}(x), v) + \Gamma(1-\alpha)(f_n, v), \quad \forall\, v \in V^{(n)}, \tag{3.3}$$

where $f_n := f(x, t_n)$, $b_k^{(n)}$ is given by (2.2), and $\widetilde{U}^{(k-1)} \in V^{(n)}$ satisfies

$$(\widetilde{U}^{(k-1)}(x), v) = (U^{(k-1)}, v), \quad \forall\, v \in V^{(n)}, \quad k = 1, \dots, n. \tag{3.4}$$

Due to the L^2 projection (3.4), scheme (3.3) is equivalent to

$$b_n^{(n)}(U^{(n)}(x),v)+\Gamma(1-\alpha)a(U^{(n)}(x),v)=\sum_{k=2}^{n}(b_k^{(n)}-b_{k-1}^{(n)})(U^{(k-1)}(x),v)\\ +b_1^{(n)}(U^{(0)}(x),v)+\Gamma(1-\alpha)(f_n,v),\quad \forall\, v\in V^{(n)}. \tag{3.5}$$

Now we present the truncation error formula for scheme (3.5). Define

$$\gamma_2^{(n)}(x):=\frac{1}{\Gamma(1-\alpha)}\sum_{k=1}^{n}b_k^{(n)}(\Delta u_k(x)-\Pi_r^{(k)}\Delta u_k(x))\\ -\frac{1}{\Gamma(1-\alpha)}\sum_{k=1}^{n}b_k^{(n)}[\Pi_r^{(k)}u(x,t_{k-1})-\Pi_r^{(k-1)}u(x,t_{k-1})], \tag{3.6}$$

and

$$\gamma_3^{(n)}:=\gamma_1^{(n)}+\gamma_2^{(n)}+O(\Delta t^2), \tag{3.7}$$

$$\gamma_4^{(n)}(x):=u(x,t_n)-u^{(n)}(x), \tag{3.8}$$

where $\Delta u_k(x):=u(x,t_k)-u(x,t_{k-1})$ and

$$u^{(n)}(x)=\Pi_r^{(n)}u(x,t_n). \tag{3.9}$$

Then we have the following lemma.

Lemma 3.1. *Let $\gamma_1^{(n)}$, $\gamma_2^{(n)}$, $\gamma_3^{(n)}$ and $\gamma_4^{(n)}$ be given by* (2.3), (3.6), (3.7) *and* (3.8), *respectively. Then the truncation error formula for scheme* (3.5) *is given by*

$$b_n^{(n)}(u^{(n)}(x),v)+\Gamma(1-\alpha)a(u^{(n)}(x),v)\\ =\sum_{k=2}^{n}(b_k^{(n)}-b_{k-1}^{(n)})(u^{(k-1)}(x),v)\\ +b_1^{(n)}(u^{(0)}(x),v)+\Gamma(1-\alpha)[(f_n,v)-(\gamma_3^{(n)}(x),v)-a(\gamma_4^{(n)}(x),v)],\quad \forall\, v\in H_0^1(I), \tag{3.10}$$

with estimation (2.13) *and*

$$|\gamma_2^{(n)}(x)|\leqslant C((h_n)^r+\Delta t^{2-\alpha}), \tag{3.11}$$

$$|\gamma_3^{(n)}(x)|\leqslant C((h_n)^r+\Delta t^{2-\alpha}), \tag{3.12}$$

$$|\gamma_4^{(n)}(x)|_{H_0^1(I)}\leqslant C((h_n)^r+\Delta t^{2-\alpha}), \tag{3.13}$$

where $h_n:=\max_{0\leqslant m\leqslant n}h^{(m)}$.

Proof. From the standard interpolation theory, it is easy to know that

$$\Delta u_k(x)=\Pi_r^{(n)}\Delta u_k(x)+O(\Delta t_n(h^{(n)})^{r+1}). \tag{3.14}$$

Using the condition on the mesh speed (3.1), we can prove that

$$\Pi_r^{(n)}u(x,t_{n-1})-\Pi_r^{(n-1)}u(x,t_{n-1})=O(\Delta t_n(h^{(n)})^r). \tag{3.15}$$

By (3.14) and (3.15) we obtain (3.11), and by (2.13) and (3.11) we derive (3.12). Again from the standard interpolation theory, we obtain the estimation (3.13). Using (3.6), we can re-write (2.1) as

$$\frac{\partial^\alpha u(x,t_n)}{\partial t^\alpha}=\frac{1}{\Gamma(1-\alpha)}\sum_{k=1}^{n}b_k^{(n)}[u^{(k)}(x)-u^{(k-1)}(x)]+\gamma_2^{(n)}(x)+\gamma_1^{(n)}(x)+O(\Delta t^2)$$

$$= \frac{1}{\Gamma(1-\alpha)}\left(b_n^{(n)}u^{(n)}(x) - \sum_{k=2}^{n}(b_k^{(n)} - b_{k-1}^{(n)})u^{(k-1)}(x) - b_1^{(n)}u^{(0)}(x)\right)$$
$$+ \gamma_2^{(n)}(x) + \gamma_1^{(n)}(x) + O(\Delta t^2). \tag{3.16}$$

Substituting $u(x,t_n) = u^{(n)}(x) + \gamma_4^{(n)}(x)$ and (3.16) into (3.2) gives the truncation error formula (3.10). □

We are now ready to show the stability of the moving finite element method (3.5).

Theorem 3.2. *Let $U^{(0)}(x) \in V^{(0)}$ and $U^{(n)}(x) \in V^{(n)}$, $n = 1,2,\ldots,L$, be generated by* (3.5) *with $f_n \equiv 0$. Then we have*

$$\|U^{(n)}(x)\| \leqslant \|U^{(0)}(x)\|, \quad n = 1,2,\ldots,L. \tag{3.17}$$

Proof. Taking $v = U^{(n)}(x)$ in (3.5) and noting that $a(U^{(n)}(x), U^{(n)}(x)) \geqslant 0$ and $f_n = 0$, we have

$$b_n^{(n)}(U^{(n)}(x), U^{(n)}(x)) \leqslant \sum_{k=2}^{n}(b_k^{(n)} - b_{k-1}^{(n)})(U^{(k-1)}(x), U^{(n)}(x)) + b_1^{(n)}(U^{(0)}(x), U^{(n)}(x))$$
$$\leqslant \sum_{k=2}^{n}(b_k^{(n)} - b_{k-1}^{(n)})\|U^{(k-1)}(x)\|\|U^{(n)}(x))\| + b_1^{(n)}\|U^{(0)}(x)\|\|U^{(n)}(x))\|. \tag{3.18}$$

Therefore,

$$b_n^{(n)}\|U^{(n)}(x)\| \leqslant \sum_{k=2}^{n}(b_k^{(n)} - b_{k-1}^{(n)})\|U^{(k-1)}(x)\| + b_1^{(n)}\|U^{(0)}(x)\|. \tag{3.19}$$

Then (3.17) follows from Lemma 2.4. □

Now we present the error estimation of the moving finite element method.

Theorem 3.3. *Let $U^{(0)}(x) \in V^{(0)}$ and $U^{(n)}(x) \in V^{(n)}$, $n = 1,2,\ldots,L$, be generated by* (3.5). *Then we have*

$$\|\eta^{(n)}(x)\| \leqslant \|\eta^{(0)}(x)\| + C((h_n)^r + \Delta t^{2-\alpha}), \quad n = 1,2,\ldots,L, \tag{3.20}$$

where $\eta^{(n)}(x) := U^{(n)}(x) - u^{(n)}(x)$. Furthermore, we have

$$\|e^{(n)}(x)\| \leqslant \|\mathrm{e}^{(0)}(x)\| + C((h_n)^r + \Delta t^{2-\alpha}), \quad n = 1,2,\ldots,L, \tag{3.21}$$

where $e^{(n)}(x) := u(x,t_n) - U^{(n)}(x)$.

Proof. Taking $v = \eta^{(n)}(x)$ in (3.10) and (3.5), and substracting (3.10) from (3.5), we have

$$b_n^{(n)}\|\eta^{(n)}\|^2 + \Gamma(1-\alpha)|\eta^{(n)}|^2_{H_0^1(I)}$$
$$= \sum_{k=2}^{n}(b_k^{(n)} - b_{k-1}^{(n)})(\eta^{(k-1)}, \eta^{(n)}) + b_1^{(n)}(\eta^{(0)}, \eta^{(n)}) + (\gamma_3^{(n)}, \eta^{(n)}) + a(\gamma_4^{(n)}, \eta^{(n)})$$
$$\leqslant \sum_{k=2}^{n}(b_k^{(n)} - b_{k-1}^{(n)})\frac{\|\eta^{(k-1)}\|^2 + \|\eta^{(n)}\|^2}{2} + b_1^{(n)}\frac{\|\eta^{(0)}\|^2 + \|\eta^{(n)}\|^2}{2}$$
$$+ \Gamma(1-\alpha)\frac{\|\gamma_3^{(n)}\|^2\lambda + \|\eta^{(n)}\|^2/\lambda}{2} + \Gamma(1-\alpha)\frac{|\gamma_4^{(n)}|^2_{H_0^1(I)} + |\eta^{(n)}|^2_{H_0^1(I)}}{2}, \tag{3.22}$$

where λ is an arbitrary positive and $|\eta^{(n)}|_{H_0^1(I)} = \sqrt{a(\eta^{(n)}, \eta^{(n)})}$ is the semi-norm of $\eta^{(n)}$ in $H_0^1(I)$. Since $\eta^{(n)} \in H_0^1(I)$, by Poincaré-Friedrichs inequalities (see e.g., [1]), we can choose a positive λ depending on the interval I such that

$$\|\eta^{(n)}\|^2/\lambda \leqslant |\eta^{(n)}|^2_{H_0^1(I)}.$$

Combining (3.22) with (3.12) and (3.13), we obtain

$$b_n^{(n)}\|\eta^{(n)}(x)\|^2 \leqslant \sum_{k=2}^{n}(b_k^{(n)} - b_{k-1}^{(n)})\|\eta^{(k-1)}(x)\|^2 + b_1^{(n)}\|\eta^{(0)}(x)\|^2 + \Gamma(1-\alpha)(\lambda\|\gamma_3^{(n)}\|^2 + \gamma_4^{(n)}|^2_{H_0^1(I)})$$

$$\leqslant \sum_{k=2}^{n}(b_k^{(n)} - b_{k-1}^{(n)})\|\eta^{(k-1)}(x)\|^2 + b_1^{(n)}\|\eta^{(0)}(x)\|^2 + C(\Delta t^{4-2\alpha} + (h_n)^{2r}). \tag{3.23}$$

From Lemma 2.4, we have

$$\begin{aligned}\|\eta^{(n)}(x)\|^2 &\leqslant \|\eta^{(0)}(x)\|^2 + C(\Delta t^{4-2\alpha} + (h_n)^{2r})/b_1^{(n)} \\ &\leqslant \|\eta^{(0)}(x)\|^2 + CT^{\alpha}(\Delta t^{4-2\alpha} + (h_n)^{2r}),\end{aligned} \tag{3.24}$$

where the last inequality is by (2.6), which proves (3.20). Consequently, it follows from the triangle inequality and (3.9) that

$$\begin{aligned}\|e^{(n)}\| &= \|u(x,t_n) - U^n(x)\| \\ &\leqslant \|u(x,t_n) - u^{(n)}(x)\| + \|u^{(n)}(x) - U^n(x)\| \\ &= \|u(x,t_n) - \Pi_r^{(n)}u(x,t_n)\| + \|\eta^{(n)}(x)\|.\end{aligned} \tag{3.25}$$

Using standard interpolation theory and (3.20), we prove (3.21) from (3.25). □

Remark 3.4. Theorem 3.3 shows that the convergence rate of the moving finite element methods is $O((h_n)^r)$ for space variable, while Jiang and Ma [9] proved that the convergence rate of finite element methods on fixed spatial grids is $O(h^{r+1})$. (In fact, combining Lemma 2.5 and [9], the convergence order can reach $O(h^{r+1}) + O(\Delta t^{2-\alpha})$ if we use the nonuniform temporal mesh as well as the uniform space mesh.) The reason for losing one order of the convergence for moving finite element methods is that the L^2 projections (3.4) from finite element spaces $V^{(k)},\ k = 0,\dots,n-1$ to space $V^{(n)}$ cause additional errors. It is hopeful to improve the convergence rates using higher-order interpolation between spaces $V^{(k)}$ and $V^{(n)}$, which is not investigated in this paper.

Remark 3.5. From the proof of Theorem 3.2, we can easily know that

$$\|u(x,t_n) - U^{(n)}\| \leqslant \|\eta^{(0)}(x)\| + C\max_{1\leqslant j\leqslant n}\mathrm{error}_j + \|u(x,t_n) - \Pi_r^{(n)}u(x,t_n)\|,$$

where error_j is the one determined by $\gamma_1^{(j)}$, $\gamma_2^{(j)}$ and $\gamma_4^{(j)}$. When the solutions have sharp variations in regions, we can choose meshes to make the above error bounds as small as possible. A natural way to do this is using moving meshes on which the interpolation errors of the solutions are as small as possible (see [8] and references therein). Thus using moving meshes helps to achieve better convergence when the solutions have sharp variations in regions.

4 Numerical examples

In this section, we provide four examples: the first one is used to test the convergence rates of the finite element method based on the nonuniform grids in time and uniform meshes in space; the second one to make comparison of convergence results between uniform grids and nonuniform ones in time; the third one to make comparison of convergence results between uniform meshes and nonuniform meshes in space and test the convergence order of the moving mesh method; and the fourth one to simulate the blow-up solutions to some time FPDEs.

In the test, the finite element method is based on the finite spaces of the 3rd-order piecewise polynomials on grid $\{x_k^{(n)}\}_{k=0}^N$. The finite spaces of polynomials of degree less than or equal to three on grid $\{x_k\}_{k=0}^N$ are constructed by

$$V_h = \left\{\sum_{k=1}^{3N-1} v_k\phi_{k/3},\ v_k \in \mathbb{R}, k = 1,\dots,3N-1\right\},$$

where $\phi_{k/3}$, $k = 1,\dots,3N-1$, are basis functions defined in the following way: let $x_{k+1/3} = x_k + (x_{k+1} - x_k)/3$, $x_{k+2/3} = x_k + 2(x_{k+1} - x_k)/3$ and denote $l_{k,j}(x),\ j = 0,1,2,3$, the basis functions of the cubic

Lagrange interpolation with respect to points x_k, $x_{k+1/3}$, $x_{k+2/3}$, x_{k+1} and

$$\phi_k = \begin{cases} l_{k-1,3}(x), & x \in [x_{k-1}, x_k], \\ l_{k,0}(x), & x \in [x_k, x_{k+1}], \\ 0, & \text{otherwise}, \end{cases} \qquad k = 1, \dots, N-1;$$

$$\phi_{k+j/3} = \begin{cases} l_{k,j}(x), & x \in [x_k, x_{k+1}], \\ 0, & \text{otherwise}, \end{cases} \qquad j = 1, 2, \quad k = 0, 1, \dots, N-1.$$

The moving meshes, based on which the moving finite element method is carried out, are generated by solving the MMPDE6

$$-\frac{\partial^2 \dot{x}}{\partial \xi^2} = \frac{1}{\tau} \frac{\partial}{\partial \xi} \left(M \frac{\partial x}{\partial \xi} \right) \tag{4.1}$$

(see e.g., [6]). In the test, the numerical solutions to MMPDE6 are approximated with the use of the central difference method for the spatial derivatives and the backward Euler method for the time derivatives.

Example 4.1. Consider

$$\frac{\partial^\alpha u}{\partial t^\alpha} - \frac{\partial^2 u}{\partial x^2} = f(x,t), \quad (x,t) \in [0,1] \times [0,1], \tag{4.2}$$

where

$$f(x,t) = 100 \sin(2\pi x) \left(\frac{\Gamma(3)}{\Gamma(3-\alpha)} t^{2-\alpha} - \frac{\Gamma(2)}{\Gamma(2-\alpha)} t^{1-\alpha} \right) + 400(t-0.5)^2 \pi^2 \sin(2\pi x),$$

with the initial condition $u_0(x) = 25 \sin(2\pi x)$ and homogeneous boundary conditions. The exact solution to the problem is given by

$$u(x,t) = 100(t-0.5)^2 \sin(2\pi x).$$

Here, uniform spatial grids and nonuniform temporal meshes are used in the computations. The temporal meshes are taken as

$$t_k = \begin{cases} \left(\frac{k}{L}\right)^2 \frac{T}{2}, & k = 1, 2, \dots, \frac{L}{2} + 1, \\ \frac{T}{2} + \left(1 - \left(\frac{k}{L}\right)^2\right) \frac{T}{2}, & k = \frac{L}{2} + 1, \dots, L+1, \end{cases} \tag{4.3}$$

and space grids are $x_k := kh,\ k = 0, \dots, N$ with $h = 1/N$. The numerical results are listed in Tables 1–2, where

$$e^{(n)} := u(x, t_n) - U^{(n)}(x),$$

and the rates of the convergence are computed by

$$\text{Rate for space} = \left| \frac{\ln(\|\text{Error on finer grid}\| / \|\text{Error on coarser grid}\|)}{\ln(N \text{ of finer grid}/N \text{ of coarser grid})} \right|,$$

$$\text{Rate for time} = \left| \frac{\ln(\|\text{Error on finer grid}\| / \|\text{Error on coarser grid}\|)}{\ln(L \text{ of finer grid}/L \text{ of coarser grid})} \right|.$$

The tables show that the convergence rate for space is 4 and the convergence rate for time is $2 - \alpha$.

Example 4.2. Consider problem (4.2) with

$$f(x,t) = [\Gamma(1+\alpha) + 4\pi^2 t^\alpha] \sin(2\pi x),$$

and initial condition $u_0(x) = 0$ and homogeneous boundary conditions. The exact solution to the problem is given by

$$u(x,t) = t^\alpha \sin(2\pi x).$$

Table 1 Convergence rate for space for Example 4.1 with $\alpha = 0.5$ and $L = 20000$

N	10	15	20	25
$\max_n \|e^{(n)}\|_\infty$	2.1305×10^{-3}	4.2703×10^{-4}	1.3516×10^{-4}	5.5895×10^{-5}
$\max_n \|e^{(n)}\|$	4.5864×10^{-4}	9.0742×10^{-5}	2.8709×10^{-5}	1.1745×10^{-5}
Conv. rate	–	3.9960	4.0001	4.0052
N	30	35	40	
$\max_n \|e^{(n)}\|_\infty$	2.7013×10^{-5}	1.4603×10^{-5}	8.5568×10^{-6}	
$\max_n \|e^{(n)}\|$	5.6501×10^{-6}	3.0364×10^{-6}	1.7678×10^{-6}	
Conv. rate	4.0139	4.0283	4.0510	

Table 2 Convergence rate for time for Example 4.1 with $\alpha = 0.5$ and $N = 100$

L	100	200	400	800
$\max_n \|e^{(n)}\|_\infty$	3.0032×10^{-3}	1.0859×10^{-3}	3.9002×10^{-4}	1.3943×10^{-4}
$\max_n \|e^{(n)}\|$	2.1236×10^{-3}	7.6788×10^{-4}	2.7579×10^{-4}	9.8596×10^{-5}
Conv. rate	–	1.4675	1.4773	1.4840
L	1600	3200	6400	
$\max_n \|e^{(n)}\|_\infty$	4.9691×10^{-5}	1.7671×10^{-5}	6.2748×10^{-6}	
$\max_n \|e^{(n)}\|$	3.5136×10^{-5}	1.2495×10^{-5}	4.4370×10^{-6}	
Conv. rate	1.4886	1.4916	1.4938	

Since the derivative of the solution is singular at $t = 0$, we take the graded grids in time as

$$t_k = \left(\frac{k}{L}\right)^4 T, \quad k = 0, 1, \dots, L, \tag{4.4}$$

and again take uniform space meshes $\{x_k\}_{k=0}^N$ with mesh size $h = 1/N$. Table 3 shows that the errors of the finite element method on graded grids in time are much smaller than those on uniform temporal grids. In this example, the errors are measured in infinity norm.

Example 4.3. Consider problem (4.2) with

$$f(x,t) = \frac{\Gamma(3)}{\Gamma(3-\alpha)} t^{2-\alpha}(\mathrm{e}^{-\frac{(x-0.5)^2}{\epsilon}} - \mathrm{e}^{-\frac{0.5^2}{\epsilon}}) + t^2 \left(\frac{2}{\epsilon}\mathrm{e}^{-\frac{(x-0.5)^2}{\epsilon}} - \frac{4(x-0.5)^2}{\epsilon^2}\mathrm{e}^{-\frac{(x-1/2)^2}{\epsilon}}\right),$$

subject to initial condition $u_0(x) = 0$ and homogeneous boundary conditions, where $\epsilon = 0.0001$. The exact solution to the problem is

$$u(x,t) = t^2(\mathrm{e}^{-\frac{(x-0.5)^2}{\epsilon}} - \mathrm{e}^{-\frac{0.5^2}{\epsilon}}).$$

Table 4 lists the convergence results obtained on uniform space meshes and those on moving meshes respectively. It shows that the approximations obtained on moving meshes are better than those obtained on uniform space meshes (the solution u has sharp variations near $x = 0.5$ when t goes larger). Here we take uniform time grid, and the space meshes are generated by solving MMPDE6 (4.1) with $\tau = 0.1$,

$$M = \sqrt{1 + u_x^2}.$$

In the computation, the monitor functions are smoothed ten times by the following schedule,

$$M_i = (3M_{i-1} + 4M_i + 3M_{i+1})/10.$$

Table 5 lists data showing the convergence order. The uniform time grid is used and the space meshes are generated in the following way: obtain the initial moving mesh ($N = 50$) by solving MMPDE6 (4.1), and generate meshes for $N = 100, 150, 200, \ldots$, by dividing every initial space interval into $2, 3, 4, \ldots$ equal parts respectively. The data in Table 5 show that the space convergence order of the moving mesh method is 4, one order higher than that in our theoretical analysis.

Example 4.4. Consider

$$\frac{\partial^\alpha u}{\partial t^\alpha} - \frac{\partial^2 u}{\partial x^2} = u^p, \quad (x,t) \in [0,1] \times [0,T] \tag{4.5}$$

with initial condition $u_0(x) = 20\sin(\pi x)$ and homogeneous boundary conditions.

In this example we use moving mesh methods to simulate the blow-up solutions. The time step sizes are determined by

$$\Delta t_n = \frac{\nu}{(\max_x u(x, t_{n-1}))^\gamma}, \tag{4.6}$$

with $\gamma = (p-\alpha)/\alpha$ and ν being a positive constant. The space meshes are generated by solving MMPDE6 (4.1) with $M = u$, $\tau = 100\Delta t_n$ for generating space grids at t_n level. The simulation results are drawn in Figures 1–3 for $\alpha = 0.5$ with $p = 2, 3, 4$.

Table 3 Comparisons of convergence results between uniform and graded grids in time with $\alpha = 0.5$ and $N = 100$ when solution u has a singularity at $t = 0$

L	500	1000	2000
$\max_n \|e^{(n)}\|_\infty$ on uniform mesh	3.7421×10^{-3}	3.2217×10^{-3}	2.6923×10^{-3}
$\max_n \|e^{(n)}\|_\infty$ on graded mesh	1.3279×10^{-5}	4.7802×10^{-5}	1.7123×10^{-6}

Table 4 Comparisons of convergence results between uniform and moving meshes in space with $\alpha = 0.5$ and $L = 8000$

N	50	80	110	140
$\max_n \|e^{(n)}\|_\infty$ on uniform mesh	8.8546×10^{-2}	7.0615×10^{-3}	1.2664×10^{-3}	9.0356×10^{-4}
$\max_n \|e^{(n)}\|_\infty$ on moving mesh	2.9521×10^{-3}	7.3699×10^{-5}	2.6463×10^{-5}	1.1533×10^{-5}

Table 5 Test of convergence order for moving mesh method with $\alpha = 0.5$ and $L = 2000$

N	50	100	150	200	250	300
$\max_n \|e^{(n)}\|_\infty$	1.35×10^{-2}	3.28×10^{-4}	9.37×10^{-5}	3.68×10^{-5}	1.66×10^{-5}	8.45×10^{-6}
$\max_n \|e^{(n)}\|$	4.95×10^{-3}	3.32×10^{-5}	8.97×10^{-6}	2.89×10^{-6}	1.19×10^{-6}	5.77×10^{-7}
Conv. rate	–	7.22	3.23	3.94	3.97	3.98

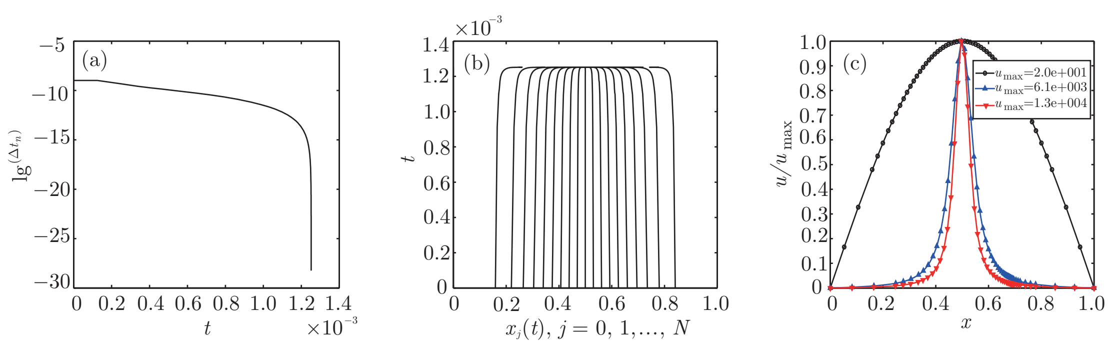

Figure 1 For Example 4.4 with $\alpha = 0.5, p = 2$. (a) t vs lg(Δt_n); (b) moving mesh trajectory $x_j(t)$; (c) for the scaled blow-up profiles

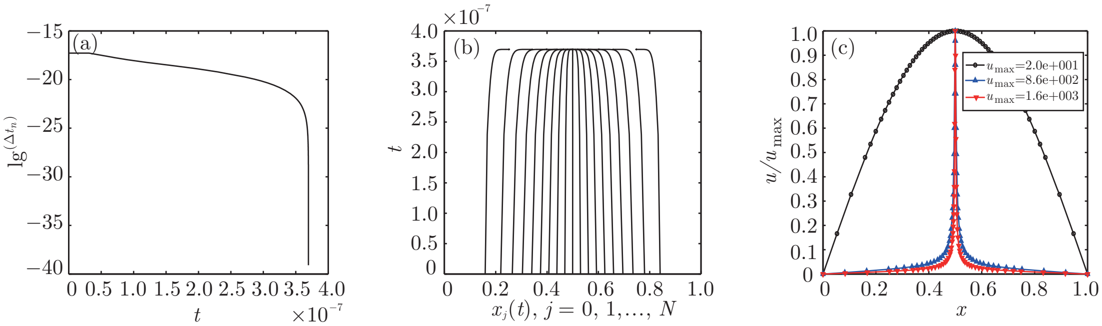

Figure 2 For Example 4.4 with $\alpha = 0.5, p = 3$. (a) t vs $\lg(\Delta t_n)$; (b) for moving mesh trajectory $x_j(t)$; (c) for the scaled blow-up profiles

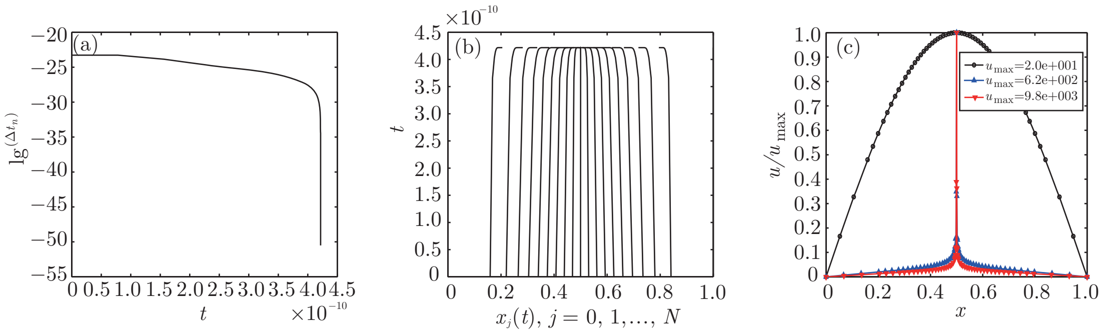

Figure 3 For Example 4.4 with $\alpha = 0.5, p = 4$. (a) t vs $\lg(\Delta t_n)$; (b) for moving mesh trajectory $x_j(t)$; (c) for the scaled blow-up profiles

5 Conclusions

In this paper, we proposed a moving finite element method to solve time fractional partial differential equations and proved the stability and convergence rates. Then we used the method to simulate blow-up solutions to some nonlinear time FPDE. Although the method theoretically has one-order lower convergence than that of the fixed finite element methods as discussed in Remark 3.4, the moving finite element method is unconditionally stable and can be used to solve the blow-up problems effectively. In the future we will further study the stability and convergence of moving finite element methods with higher-order interpolations at different levels of finite element spaces and the stability and convergence of discontinuous Galerkin methods (see e.g., [14, 20]).

Acknowledgements This work was supported by National Natural Science Foundation of China (Grant Nos. 10901027 and 11171274) and Foundation of Hunan Educational Committee (Grant No. 10C0370).

References

1 Brenner S C, Scott L R. The Mathematical Theory of Finite Element Methods. New York: Springer-Verlag, 2002

2 Chen C, Liu F, Turner I, et al. A fourier method for the fractional diffusion equation describing sub-diffusion. J Comput Phys, 2007, 227: 886–897

3 Diethelm K, Ford N J, Freed A D. A predictor-corrector approach for the numerical solution of fractional differential equations. Nonlinear Dynam, 2002, 29: 3–22

4 Diethelm K, Ford N J, Freed A D. Detailed error analysis for a fractional Adams method. Numer Algorithm, 2004, 36: 31–52

5 Gorenflo R, Mainardi F. Some recent advances in theory and simulation of fractional diffusion processes. J Comput Appl Math, 2009, 229: 400–415

6 Huang W, Ren Y, Russell R D. Moving mesh partial differential equations (MMPDEs) based upon the equidistribution principle. SIAM J Numer Anal, 1994, 31: 709–730

7 Huang W, Russell R D. Adaptive Moving Mesh Methods. New York: Springer-Verlag, 2011

8 Huang W Z, Sun W W. Variational mesh adaptation II: error estimates and monitor functions. J Comput Phys, 2003, 184: 619–648

9 Jiang Y J, Ma J T. High-order finite element methods for time-fractional partial differential equations. J Comput Appl Math, 2011, 235: 3285–3290

10 Kirane M, Laskri Y, Tatar N E. Critical exponents of Fujita type for certain evolution equations and systems with spatio-temporal fractional derivatives. J Math Anal Appl, 2005, 312: 488–501

11 Li C, Deng W. Remarks on fractional derivatives. Appl Math Comput, 2007 187: 777–784

12 Li X J, Xu C J. A space-time spectral method for the time fractional diffusion equation. SIAM J Numer Anal, 2009 47: 2108–2131

13 Lin Y M, Xu C J. Finite difference/spectral spproximations for the time-fractional diffusion equation. J Comput Phys, 2007, 225: 1533–1552

14 Liu Y X, Shu C W. Error analysis of the semi-discrete local discontinuous Galerkin method for semiconductor device simulation models. Sci China Math, 2010, 12: 3255–3278

15 Lubich C. Discretized fractional calculus. SIAM J Math Anal, 1986, 17: 704–719

16 Ma J T, Jiang Y J. Moving collocation methods for time fractional differential equations and simulation of blowup. Sci China Math, 2011, 54: 611–622

17 McLean W, Mustapha K. Convergence analysis of a discontinuous Galerkin method for a sub-diffusion equation. Numer Algorithm, 2009, 5: 69–88

18 Metzler R, Klafter J. The random walk's guide to anomalous diffusion: a fractional dynamics approach. Phys Rep, 2000, 339: 1–77

19 Mustapha K, McLean M. Piecewise-linear, discontinous Galerkin method for a fractional diffusion equation. Numer Algorithm, 2011, 56: 159–184

20 Yang J M, Chen Y P. A priori error analysis of a discontinuous Galerkin approximation for a kind of compressible miscible displacement problems. Sci China Math, 2010, 10: 2679–2696

21 Zhuang P, Liu F, Anh V, et al. New solution and analytical techniques of the implicit numerical method for the anomalous subdiffusion equation. SIAM J Numer Anal, 2008, 46: 1079–1095

22 Zhuang P, Liu F, Anh V, et al. Stability and convergence of an implicit numerical method for the non-linear fractional reaction-subdiffusion process. IMA J Numer Math, 2009, 74: 645–667